Absence of Chiral Molecular Recognition in Irregular Linear and Macrocyclic Liquid Crystalline Polyethers Based on 1-(4-Hydroxy-4′-biphenylyl)-2-(4-hydroxyphenyl)butane and α,ω-Dibromoalkanes[1a]

Virgil Percec* and Masaya Kawasumi

Department of Macromolecular Science, Case Western Reserve University, Cleveland, Ohio 44106-2699

Received January 15, 1993; Revised Manuscript Received April 22, 1993

ABSTRACT: This paper describes the synthesis and characterization of chiral (*R*)-1-(4-hydroxy-4′-biphenylyl)-2-(4-hydroxyphenyl)butane [(*R*)-TPB], of its irregular linear polyethers with α,ω-dibromoalkanes [(*R*)-TPB-(l)*X*, where *X* is the number of methylene groups in the spacer, i.e., *X* = 10, 12, 14, and 16], and of its irregular macrocyclics with 1,10-dibromodecane [(*R*)-TPB-(c)10(*z*), where *z* is the degree of oligomerization of the macrocyclic, i.e., *z* = 1–5 are monomer to pentamer]. The phase behavior of chiral linear and macrocyclic derivatives was compared to that of their racemic homologues. Both linear and macrocyclic chiral compounds display a cholesteric mesophase while the corresponding racemic derivatives a nematic mesophase. All thermal transition temperatures of the chiral and racemic linear polymers are identical. The isotropization temperatures of the chiral and racemic macrocyclics are also identical. However, the melting transitions of chiral macrocyclics are higher than those of the racemic derivatives. This behavior was explained by the absence of chiral molecular recognition of the structural units derived from the two enantiomers which is most probably due to the irregular microstructure of the two series of compounds. The UV and CD spectra of chiral linear and cyclic compounds are identical in solution. However, the CD spectra of macrocyclics obtained from their cholesteric phase are strongly dependent on ring size. It has been suggested that a supercoiled suprastructure in the cholesteric phase may be responsible for the behavior of macrocyclics.

Introduction

Liquid crystallinity and chirality have received considerable interest both for pure scientific and for technologically driven reasons.[1b–5] This is mostly because of the interesting physical properties exhibited by chiral liquid crystals. Reflection of polarized light by cholesteric mesophases,[3] ferroelectric, ferrielectric, and antiferroelectric properties exhibited by S_C^* phases,[4] piezoelectric properties displayed by chiral liquid crystalline networks,[5] and separation of enantiomers by capillary column gas chromatography using chiral liquid crystalline polymers as stationary phases[6] are only some of them. Most of these properties are determined by the unique helical supramolecular structure of various chiral mesophases. In chiral polymeric systems, the chirality of the individual structural units may be enhanced due to the helical conformation of the backbone through a cooperative effect among the chiral monomeric units.[7]

The introduction of chiral groups into a nematic polymer by either copolymerization or physical mixing with low or high molecular weight chiral molecules induces the twisting of the nematic director, thus generating a cholesteric phase. There are many reports on the synthesis of main chain cholesteric homopolymers and copolymers which are prepared mostly by using a mesogenic unit and a chiral flexible spacer,[8a–f] with one exception in which the chiral group was pendant to the mesogenic group.[8g] One of the interesting properties of cholesteric materials is that, under certain conditions, they exhibit selective reflection of the polarized light whose wavelength is determined by the helical pitch of the cholesteric phase. The helical pitch can be controlled either by external conditions such as temperature or via structural factors such as the composition of chiral and nonchiral monomers. Therefore, indirectly, the wavelength of the polarized light or the helical pitch can provide important structural information about the supramolecular architecture of a certain system.

Recently, we have reported the synthesis and characterization of irregular linear polyethers based on 1-(4-hydroxy-4′-biphenylyl)-2-(4-hydroxyphenyl)butane (TPB) and α,ω-dibromoalkanes containing from four to twenty methylene units [TPB-(l)*X*, where *X* is the number of methylene units in the spacer].[9a,b] All TPB-(l)*X* polyethers are soluble in conventional solvents and, therefore, can be prepared with well-defined molecular weights and chain ends. In addition, depending on their spacer length these polymers exhibit glassy, noncrystallizable enantiotropic nematic, enantiotropic crystallizable nematic, and monotropic and virtual nematic mesophases.[9a,b] Presently, these polymers are used as model systems for various physical investigations.[9d,e] In addition, TPB and α,ω-dibromoalkanes were used for the elaboration of a novel class of molecular liquid crystals, i.e., macrocyclic liquid crystals.[10] TPB contains a chiral carbon atom. However, all investigations performed so far on the linear and macrocyclic derivatives of TPB were carried out with the racemic derivative.

The first goal of this paper is to describe the synthesis of chiral (*R*)-1-(4-hydroxy-4′-biphenylyl)-2-(4-hydroxyphenyl)butane [(*R*)-TPB], of its irregular linear polyethers with α,ω-dibromoalkanes (*R*)-TPB-(l)*X* (with *X* = 10, 12, 14, and 16), and of its irregular macrocyclics with α,ω-dibromodecane (*R*)-TPB-(c)10(*z*) [where *z* is the degree of oligomerization of the macrocyclic, i.e., *z* = 1 (monomer), 2 (dimer), 3 (trimer), etc.]. The second goal of this paper is to provide a quantitative comparison of the phase behavior of TPB-(l)*X* and (*R*)-TPB-(l)*X* and of TPB-(c)10(*z*) and (*R*)-TPB-(c)10(*z*). This is the first study which discusses quantitatively, with well-defined samples, the phase behavior of racemic and chiral linear polymers and macrocyclics oligomers.

* To whom all correspondence should be addressed.

0024-9297/93/2226-3917$04.00/0

Experimental Section

Materials. Thionyl chloride, lithium aluminum hydride ($LiAlH_4$, 95+%), tetrabutylammonium hydrogen sulfate (TBAH, 97%), 4-methoxyphenylacetic acid (99%), (−)-cinchonidine (98%) (all from Aldrich), anhydrous $AlCl_3$, 48% HBr (both from Fisher Scientific), iodoethane (Lancaster Synthesis), naphthalene (Matheson Coleman & Bell), and acetic anhydride (J. T. Baker Chemical Co.) were used as received. 1,10-Dibromodecane (97%) (Aldrich) was purified by vacuum distillation. 1,12-Dibromododecane (Lancaster Synthesis) and 1,16-dibromohexadecane (Pfaltz & Bauer) were recrystallized from methanol. 1,14-Dibromotetradecane was synthesized as described in a previous publication.[11] Tetrahydrofuran (THF) and diethyl ether were dried by refluxing over $LiAlH_4$ and were freshly distilled from $LiAlH_4$ before use. Methylene chloride and chloroform were refluxed over CaH_2 and then were distilled from CaH_2. *o*-Dichlorobenzene was distilled under reduced pressure. 4-Acetoxybiphenyl was synthesized as described elsewhere.[9a] All other chemicals were commercially available and were used as received.

Synthesis of (*R*)-1-(4-hydroxy-4′-biphenylyl)-2-(4-hydroxyphenyl)butane [(*R*)-9] is outlined in Scheme I.

Synthesis of 2-(4-Methoxyphenyl)butanoic Acid. Alkylation of 4-methoxyphenylacetic acid (1) with iodoethane was carried out according to a literature procedure.[12] Naphthalene (55.4 g, 0.432 mol) was dissolved in 250 mL of dry THF. After the addition of sodium (10.5 g, 0.457 mol), the mixture was stirred for 8 h at room temperature under nitrogen. The obtained sodium naphthalide–THF solution was added carefully (an exothermic reaction takes place), to a vigorously stirred solution of 4-methoxyphenylacetic acid (1, 31.1 g, 0.188 mol) in 250 mL of dry THF. After the solution was stirred for 3 h at room temperature, iodoethane was added dropwise via a dropping funnel over 12 min and the mixture was stirred at room temperature overnight. Water (90 mL) was added to the reaction mixture. The sodium salt of the alkylated acid was extracted with 180 mL of a 10% Na_2CO_3 aqueous solution and 400 mL of water, successively. The layer was washed two times with 200 mL of diethyl ether and then was acidified with hydrochloric acid. The resulting free acid was extracted with diethyl ether, and the solution was dried over $MgSO_4$. The solvent was evaporated to yield a liquid which was distilled under reduced pressure. Crystallization from hexanes yielded white crystals (28.7 g, 78.6%): mp 66–68 °C (lit.[12] mp 51–58 °C); ^{1}H-NMR ($CDCl_3$, TMS, δ, ppm) 0.89 (3H, CH_3–CH_2–, t, J = 7.1 Hz), 1.77 and 2.08 (2H, –CH_2–, 2m), 3.40 (1H, –CH–COOH, t, J = 7.1 Hz), 3.78 (3H, CH_3O–, s), 6.86 (2H, ortho to the methoxy, d, J = 8.3 Hz), 7.24 (2H, meta to the methoxy, d, J = 8.2 Hz).

Resolution of (*S*)-2-(4-Methoxyphenyl)butanoic Acid [(*S*)-2]. (*S*)-2-(4-Methoxyphenyl)butanoic acid [(*S*)-2] was separated by fractional recrystallization of the salts of racemic 2-(4-methoxyphenyl)butanoic acid with (−)-cinchonidine followed by the regeneration of the acid according to a literature procedure.[12] 2-(4-Methoxyphenyl)butanoic acid (28.5 g, 0.147 mol) and (−)-cinchonidine (44.1 g, 0.150 mol) were dissolved in a mixture of 95% ethanol (300 mL) and water (75 mL) and crystallized at room temperature. After filtration, 24.2 g of fibril-like crystals of the salts were obtained. The optical purity (percent enantiomeric excess, ee) monitored by the ratio of methoxy peaks (*S*-diastreomer, 3.70 ppm; *R*-diastereomer, 3.64 ppm) of the ^{1}H-NMR spectrum of the diastereomeric salt recorded in $CDCl_3$ was 44.8%. The rest of the salts remained in solution and was precipitated by adding a large amount of water. The precipitate was collected by filtration. The main fraction of salts was recrystallized from a mixture of 95% ethanol and water (first, 100 mL of ethanol/25 mL of water; second, 50 mL of ethanol/12.5 mL of water) two times to yield 8.49 g of fibril-like crystals (ee, 76%). The salts recovered from solution were also recrystallized several times until the optical purity reached about 77% ee and then was combined with the main fraction. The total yield of salt was 22.2 g (59%). The salt was dissolved in $CHCl_3$ (600 mL) and was acidified with a mixture of concentrated sulfuric acid (40 mL) and water (220 mL). The organic layer was washed two times with 300 mL of water and was dried over $MgSO_4$. After filtration followed by evaporation of the solvents, the acid was recrystallized from hexanes to yield white crystals (7.12 g, 47.6% calculated on the (*S*)-acid basis). The optical purity measured by ^{1}H-NMR spectroscopy by preparing its salt with (−)-cinchonidine directly in the NMR sample tube was 89% ee. Mp: 83–86 °C (lit.[12] mp 85–86 °C). ^{1}H-NMR ($CDCl_3$, TMS, δ, ppm): 0.89 (3H, CH_3–CH_2–, t, J = 7.1 Hz), 1.77 and 2.08 (2H, –CH_2–, 2m), 3.40 (1H, –CH–COOH, t, J = 7.1 Hz), 3.78 (3H, cH_3O–, s), 6.86 (2H, ortho to the methoxy, d, J = 8.3 Hz), 7.24 (2H, meta to the methoxy, d, J = 8.2 Hz).

Scheme I. Synthesis of (*R*)-1-(4-Hydroxy-4′-biphenylyl)-2-(4-hydroxyphenyl)butane [(*R*)-TPB]

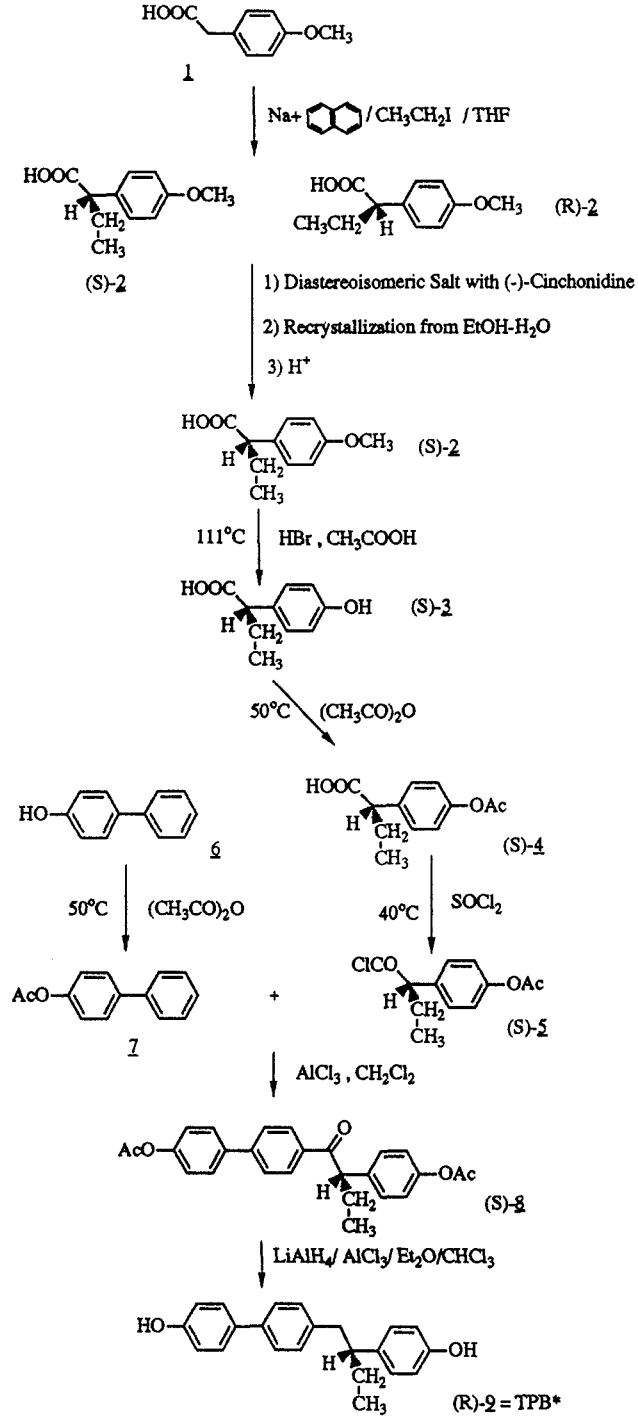

Synthesis of (*S*)-2-(4-Hydroxyphenyl)butanoic Acid [(*S*)-3]. (*S*)-2-(4-Hydroxyphenyl)butanoic acid [(*S*)-3] was prepared by the demethylation of (*S*)-2-(4-methoxyphenyl)butanoic acid [(*S*)-2] with HBr. (*S*)-2-(4-Methoxyphenyl)butanoic acid (6.86 g, 35 mmol) was dissolved in a mixture of 48% HBr (13.3 mL) and acetic acid (47 mL). The solution was heated to reflux for 23 h (reflux temperature, 111 °C) after which the reaction mixture was cooled to room temperature and 100 mL of water was added. The product was extracted two times with 100 mL of diethyl ether. The ether layer was washed two times with 100 mL of

water and then was dried over $MgSO_4$. After the evaporation of solvents, the remaining solid was recrystallized from water to yield 5.17 g (82.0%) of needlelike crystals. Mp: 136–138 °C. ^{1}H-NMR (DMSO-d_6, TMS, δ, ppm): 0.81 (3H, CH_3–CH_2–, t, J = 7.4 Hz), 1.58 and 1.91 (2H, –CH_2–, 2m), 3.24 (1H, –CH–COOH, t, J = 8.1 Hz), 6.72 (2H, ortho to the hydroxy, d, J = 7.9 Hz), 7.08 (2H, meta to the hydroxy, d, J = 9.3 Hz), 9.24 (1H, –COOH, broad peak). The ^{1}H-NMR spectrum showed that the resulting acid is free of unreacted methoxy group.

Synthesis of (*S*)-2-(4-Acetoxyphenyl)butanoic Acid [(*S*)-4]. (*S*)-2-(4-Acetoxyphenyl)butanoic acid [(S)-4] was prepared by the acetylation of (*S*)-2-(4-hydroxyphenyl)butanoic acid [(*S*)-3]. (*S*)-2-(4-Hydroxyphenyl)butanoic acid (5.04 g, 28 mmol), acetic anhydride (5.71 g, 56 mmol), and a few drops of sulfuric acid diluted with acetic anhydride were stirred at 50 °C for 1.5 h. The reaction mixture was cooled to room temperature, 25 mL of water was added, and the mixture was stirred overnight. After the addition of 200 mL of water the product was extracted with 200 mL of diethyl ether. The ether layer was washed three times with water and was dried over $MgSO_4$. After the evaporation of the solvent, it was recrystallized from water to yield 5.40 g (86.8%) of white fine crystals. Mp: 64–68 °C. ^{1}H-NMR ($CDCl_3$, TMS, δ, ppm): 0.92 (3H, CH_3–CH_2–, t, J = 7.5 Hz), 1.79 and 2.10 (2H, –CH_2–, 2m), 2.29 (3H, CH_3CO–, s), 3.46 (1H, –CH–COOH, t, J = 7.4 Hz), 7.05 (2H, ortho to the acetoxy, d, J = 9.2 Hz), 7.33 (2H, meta to the acetoxy, d, J = 8.5 Hz).

Synthesis of (*S*)-1-(4-Acetoxy-4′-biphenylyl)-2-(4-acetoxyphenyl)butanone [(*S*)-8]. A mixture of (*S*)-2-(4-acetoxyphenyl)butanoic acid [(S)-4, 5.33 g, 24 mmol], thionyl chloride (3.0 mL, 41 mmol), and a few drops of dimethylformamide was stirred for 1.5 h at room temperature under nitrogen. The excess thionyl chloride was removed under reduced pressure to yield a pale yellow liquid which was used directly in the acylation reaction. 4-Acetoxybiphenyl (7, 6.11 g, 29 mmol) was dissolved in 30 mL of dry methylene chloride and cooled to below 10 °C in an ice-water bath, after which 11.5 g (86 mmol) of anhydrous $AlCl_3$ was added. (*S*)-2-(4-Acetoxyphenyl)butanoic acid chloride [(*S*)-5] was dissolved in 30 mL of dry methylene chloride. This solution was added dropwise to a solution of 4-acetoxybiphenyl over 35 min under cooling, and the deep red solution was stirred under cooling for 50 min. Afterward it was poured into a mixture of 20 mL of concentrated HCl and 60 mL of ice water. The organic layer was separated and washed two times with water, after which it was dried over anhydrous $MgSO_4$ and filtered and the solvents were removed in a rotary evaporator to yield a viscous orange oil. The product was recrystallized from diethyl ether solution and purified by silica gel column chromatography (using a mixture of hexanes and diethyl ether as eluent). After recrystallization from ethanol, 3.2 g (32%) of white crystals was obtained. Purity (HPLC), 98.9%. Mp: 140–141 °C. ^{1}H-NMR ($CDCl_3$, TMS, δ, ppm): 0.92 (3H, CH_3–CH_2–, t, J = 7.4 Hz), 1.86 and 2.22 (2H, –CH_2–, 2m), 2.27 (3H, CH_3COO–Ph–CH–, s), 2.34 (3H, CH_3COO–biphenyl, s), 4.50 (1H, –CH–, t, J = 6.9 Hz), 7.04 (2H, ortho to acetoxy of the monophenyl ring, d, J = 9.5 Hz), 7.18 (2H, ortho to acetoxy of the biphenyl ring, d, J = 8.7 Hz), 7.35 (2H, meta to acetoxy of the monophenyl ring, d, J = 7.6 Hz), 7.59 (4H, meta to acetoxy of the biphenyl ring and meta to acyl, 2d, J = 8.5 Hz), 8.04 (2H, ortho to acyl, d, J = 8.6 Hz).

Synthesis of (*R*)-1-(4-Hydroxy-4′-biphenylyl)-2-(4-hydroxyphenyl)butane [(*R*)-9]. (*R*)-9 was prepared by the reduction of (*S*)-1-(4-acetoxy-4′-biphenylyl)-2-(4-acetoxyphenyl)-butanone [(S)-8] with $LiAlH_4$/$AlCl_3$·Et_2O complex.[9a] $AlCl_3$ (26.7 g, 200 mmol) was placed in a 100-mL three neck flask equipped with a dropping funnel, nitrogen inlet–outlet, and magnetic stirrer and cooled in an ice-water bath, after which 35 mL of dry diethyl ether was added dropwise under nitrogen. $LiAlH_4$ (1.73 g, 46 mmol) was placed in a 250-mL three neck flask equipped with dropping funnel, nitrogen inlet–outlet, and magnetic stirrer and cooled in an ice-water bath. To the flask containing $LiAlH_4$ were added successively 25 mL of dry diethyl ether, the solution of $AlCl_3$ diethyl ether complex, and 25 mL of dry chloroform. A solution of (*S*)-8 (3.17 g, 7.6 mmol) in 50 mL of dry chloroform was added dropwise to the reducing agent solution maintained at 0 °C. The resulting reaction mixture was stirred at room temperature overnight. To this mixture cooled with an ice-water bath was added dropwise a solution of 50 mL of concentrated HCl and 60 mL of water. After the reaction mixture was stirred for several hours, the product was extracted with 300 mL of chloroform. The organic layer was separated, washed two times with 300 mL of water, and dried over anhydrous $MgSO_4$. After filtration, the solvent was evaporated to give a viscous liquid. The liquid was crystallized from toluene to yield 1.61 g (66.5%) of white crystals. Purity (HPLC), 99.3%. Mp: premelting at 140–142 °C followed by crystallization and melting at 159–160 °C. ^{1}H-NMR ($CDCl_3$, TMS, δ, ppm): 0.77 (3H, –CH_3, t, J = 7.1 Hz), 1.69 (2H, CH_3–CH_2–, m), 2.68 (1H, –CH–, m), 2.85 (2H, Ph–CH_2–CH–, d of d, J = 5.8 and 8.3 Hz), 4.62 (1H, –CH–Ph–OH, s), 4.82 (1H, HO–biphenyl, s), 6.77 (2H, ortho to hydroxy of the monophenyl ring, d, J = 8.5 Hz), 6.91 (2H, ortho to hydroxy of the biphenyl ring, d, J = 9.3 Hz), 6.98 (2H, meta to hydroxy of the monophenyl ring, d, J = 8.8 Hz), 7.09 (2H, ortho to methylene of the biphenyl ring, d, J = 8.9 Hz), 7.37 (2H, meta to hydroxy of the biphenyl ring, d, J = 7.7 Hz), 7.43 (2H, meta to methylene of the biphenyl ring, d, J = 8.6 Hz).

Preparation of Chiral Linear Irregular Polyethers (*R*)-TPB-(l)*X* Based on the Chiral (*R*)-TPB [(*R*)-9] and α,ω-Dibromoalkanes. A similar procedure with that described in a previous paper[9a] was used to synthesize chiral linear (*R*)-TPB-(l)*X* polymers containing *X* (*X* = 10, 12, 14, and respectively 16) methylene units in their flexible spacer. An example of this procedure is as follows.

To a 25-mL single neck flask equipped with condenser and nitrogen inlet–outlet were successively added 0.159 g (0.50 mmol) of (*R*)-9, 1.0 mL of *o*-dichlorobenzene, 0.150 g (0.50 mmol) of 1,10-dibromodecane, 1.0 mL of 10 N NaOH, and 0.0679 g (0.20 mmol, 20 mol % of phenol groups) of TBAH. The ratio between the volume of *o*-dichlorobenzene and the total moles of monomers was maintained constant in all polymerizations. The reaction mixture was stirred at 1100 rpm with a magnetic stirrer at 80 °C under nitrogen. After 30 min of reaction, the organic and aqueous layers were diluted with chloroform and water, respectively, and the aqueous layer was separated. The organic layer was washed with water, followed by dilute hydrochloric acid, and again three times with water. The polymer was separated by the precipitation of its solution into methanol to obtain 0.226 g (98.8%) of a white fibrous precipitate. The polymer was further purified by four successive precipitations from chloroform solution, first into acetone to remove all cyclic oligomers, and then into methanol, followed by the two precipitations from THF solution into water.

Preparation of Chiral Irregular Cyclic Oligoethers [(*R*)-TPB-(c)10(*z*)] Based on the Chiral (*R*)-TPB [(*R*)-9] and 1,10-Dibromodecane [*z* Defines the Ring Size, i.e., *z* = 1 (Monomer), 2 (Dimer), 3 (Trimer), 4 (Tetramer), 5 (Pentamer)]. A similar procedure with that described in the previous paper[10a] for the preparation of corresponding racemic macrocyclics was used to synthesize the chiral (*R*)-TPB-(c)10(*z*) macrocyclics. An example is as follows.

To a 500-mL single neck flask equipped with condenser were successively added 0.318 g (1.00 mmol) of (*R*)-9, 100 mL of 10 N NaOH aqueous solution (1.0 mol), 100 mL of *o*-dichlorobenzene, 0.300 g (1.00 mmol) of 1,10-dibromodecane, and 0.136 g (0.40 mmol, 20 mol % of phenol groups) of TBAH. A balloon filled with nitrogen was placed at the top of the condenser. The reaction mixture was stirred at 1100 rpm with a magnetic stirrer at 80 °C. After 40 h, the reaction mixture was diluted with water and chloroform. The organic layer was washed two times with water, once with dilute hydrochloric acid, and three times with water. After the evaporation of the solvents, the product was dissolved in chloroform. To this solution was added silica gel, and the chloroform was evaporated. The product absorbed on silica gel was charged on the top of a column containing silica gel and was flushed with acetone to separate the mixture of cyclic oligomers. The product remaining at the top of the column was flushed with chloroform to separate the higher molecular weight part. The mixture of cyclic oligomers was separated into about 50 fractions by silica gel column chromatography using a mixture of acetone and hexanes as eluent (1:20 v/v). Each fraction was checked by TLC [developed by a mixture of acetone and hexanes (1:15–1:20 v/v) and detected with a UV lamp]. The fraction containing each cyclic oligomer was collected and the solvents were evaporated on a rotary evaporator to yield the individual cyclic oligomers. The cyclic trimer, tetramer, and pentamer were

further purified by repeating the same purification by column chromatography.

Techniques. ^{1}H-NMR (200 MHz) spectra were recorded on a Varian XL-200 NMR spectrometer. All spectra were acquired at room temperature. TMS was used as the internal standard.

Relative molecular weights and purities were determined by gel permeation chromatography (GPC) and high pressure liquid chromatography (HPLC). GPC analyses were carried out with a Perkin-Elmer series 10 LC equipped with an LC-100 column oven and a Nelson Analytical 900 series data station. The measurements were made by using the UV detector, chloroform as the solvent (1 mL/min, 40 °C), two PL gel columns of 5×10^2 and 10^4 Å, and a calibration plot constructed with polystyrene standards. HPLC analyses were performed with the same instrument with a PL gel column of 1×10^2 Å.

A Perkin-Elmer DSC-4 differential scanning calorimeter equipped with a TADS data station Model 3600 was used to determine thermal transitions. Heating and cooling rates were 20 °C/min in all cases. First-order transitions (crystalline–crystalline, crystalline–liquid crystalline, liquid crystalline–isotropic, etc.) were read at the maximum or minimum of the endothermic or exothermic peaks. Glass transition temperatures (T_g) were read at the middle of the change in the heat capacity. All heating and cooling scans after the first heating scan produced perfectly reproducible data. We will report the transitions collected from the first and second or subsequent heating scans and from the first cooling scan.

A Carl Zeiss optical polarizing microscope (magnification 50×) equipped with a Mettler FP 82 hot stage and a Mettler FP 800 central processor was used to observe thermal transitions and to analyze anisotropic textures.[13]

UV spectra were recorded on a Varian DMS 200 UV–vis spectrophotometer at room temperature. CD spectra were obtained by using a JASCO J-40A automatic recording spectropolarimeter at room temperature. The films for solid state CD measurements were prepared as follows. The sample was placed between a slide glass and a thin cover slide glass and was heated until the compound was in its liquid crystalline or isotropic phase. The thin film was obtained by pushing the cover glass without shearing. The sample was then quenched to room temperature by cooling on contact with a cold surface. The temperatures from which samples were quenched are as follows: (*R*)-TPB-(c)10(2), from above isotropization temperature; (*R*)-TPB-(c)10(3) from 82 °C; (*R*)-TPB-(c)10(4) from 108 °C; (*R*)-TPB-(c)10(5) from 104 °C; linear (*R*)-TPB-(l)10 from about 100 °C.

Results and Discussion

Synthesis of the (*R*)-TPB Monomer. Scheme I presents the synthesis of the chiral TPB [(*R*)-9]. In this scheme none of the reaction steps after the alkylation of 4-methoxyphenylacetic acid involve racemization or inversion of configuration of the chiral center. Therefore, the configuration sign of these compounds changes as indicated in Scheme I.

Figure 1 presents the ^{1}H-NMR spectra of the methoxy protons of racemic and resolved 2-(4-methoxyphenyl)-butanoic acid in the presence of an equal molar amount of (−)-cinchonidine in $CDCl_3$. Since 2-(4-methoxyphenyl)-butanoic acid forms a diastereomeric salt with (−)-cinchonidine in $CDCl_3$, the protons of (*S*)- and (*R*)-acids have different chemical shifts. Therefore, their optical purities can be monitored by measuring the intensities of the methoxy protons of the two acids, as shown in Figure 1. Three successive recrystallizations of the salt of 2-(4-methoxyphenyl)butanoic acid with (−)-cinchonidine, followed by acidification, yielded the (*S*)-2-(4-methoxyphenyl)butanoic acid with 89% ee optical purity (Figure 1). Although the optical purity of this compound could be enhanced further by increasing the number of recrystallizations, its yield would have become much lower and, therefore, we preferred to perform these experiments with the present optical purity. In the acylation step, when

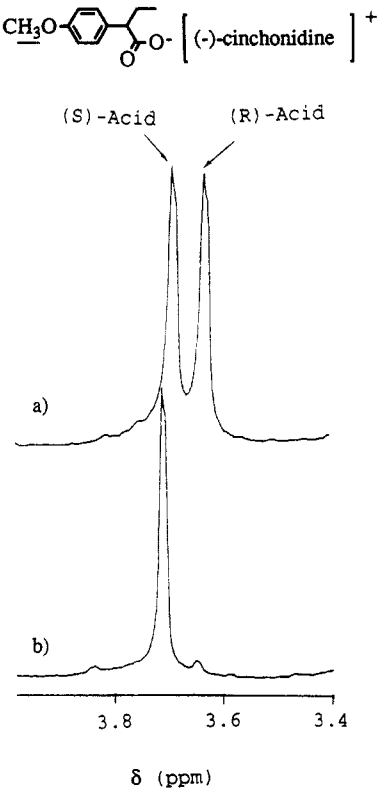

Figure 1. ^{1}H-NMR spectra of the methoxy protons of 2-(4-methoxyphenyl)butanoic acid in the presence of an equal molar amount of (−)-cinchonidine in $CDCl_3$: (a) racemic 2-(4-methoxyphenyl)butanoic acid; (b) resolved (*S*)-2-(4-methoxyphenyl)-butanoic acid.

(*S*)-2-(4-methoxyphenyl)butanoic acid and 4-methoxybiphenyl were used instead of (*S*)-2-(4-acetoxyphenyl)-butanoic acid and 4-acetoxybiphenyl, the conversion to the desired product was very low. This is most probably due to the occurrence of the acylation on the ortho positions to the methoxy groups of the phenyl ring of (*S*)-2-(4-methoxyphenyl)butanoic acid and of the biphenyl ring since these positions are activated by the methoxy group. Therefore, the acetoxy compounds were used in this reaction step.

Characterization of Chiral Irregular Linear (*R*)-TPB-(l)*X* Polymers and Cyclic (*R*)-TPB-(c)10(*z*) Oligomers. Scheme II presents the synthesis of linear polymers and that of the macrocyclics of (*R*)-TPB with α,ω-dibromoalkanes. As indicated in this scheme, both linear polymers and cyclic oligomers contain mostly the two constitutional isomers of the (*R*)-TPB stereoisomer with a minor amount of the two constitutional isomers of the (*S*)-TPB stereoisomer. Therefore, the configurational entropy of the chiral polymer backbone should be lower than that of the backbone of the racemic linear polymer. In addition, since the reactivities of the two phenolates of TPB are not very different,[9c] both the linear and macrocyclic derivatives are irregular because they contain a random distribution of the head-to-head and head-to-tail structural units derived from the two TPB enantiomers.

The characterization results of (*R*)-TPB-(l)*X* and (*R*)-TPB-(c)10(*z*) oligomers with the data of the corresponding racemic polymers and oligomers are presented in Tables I and II, respectively. Both the racemic and the chiral linear polymers and cyclic oligomers are soluble in conventional solvents such as chloroform, THF, dioxane, and methylene chloride. No difference between the solubility of racemic and chiral compounds was observed. The number average molecular weights of (*R*)-TPB-(l)*X*

Scheme II. Synthesis of Chiral Linear (*R*)-TPB-(l)*X* polymers and cyclic (*R*)-TPB-(c)10(*z*) Oligomers Based on (*R*)-TPB and α,ω-Dibromoalkanes

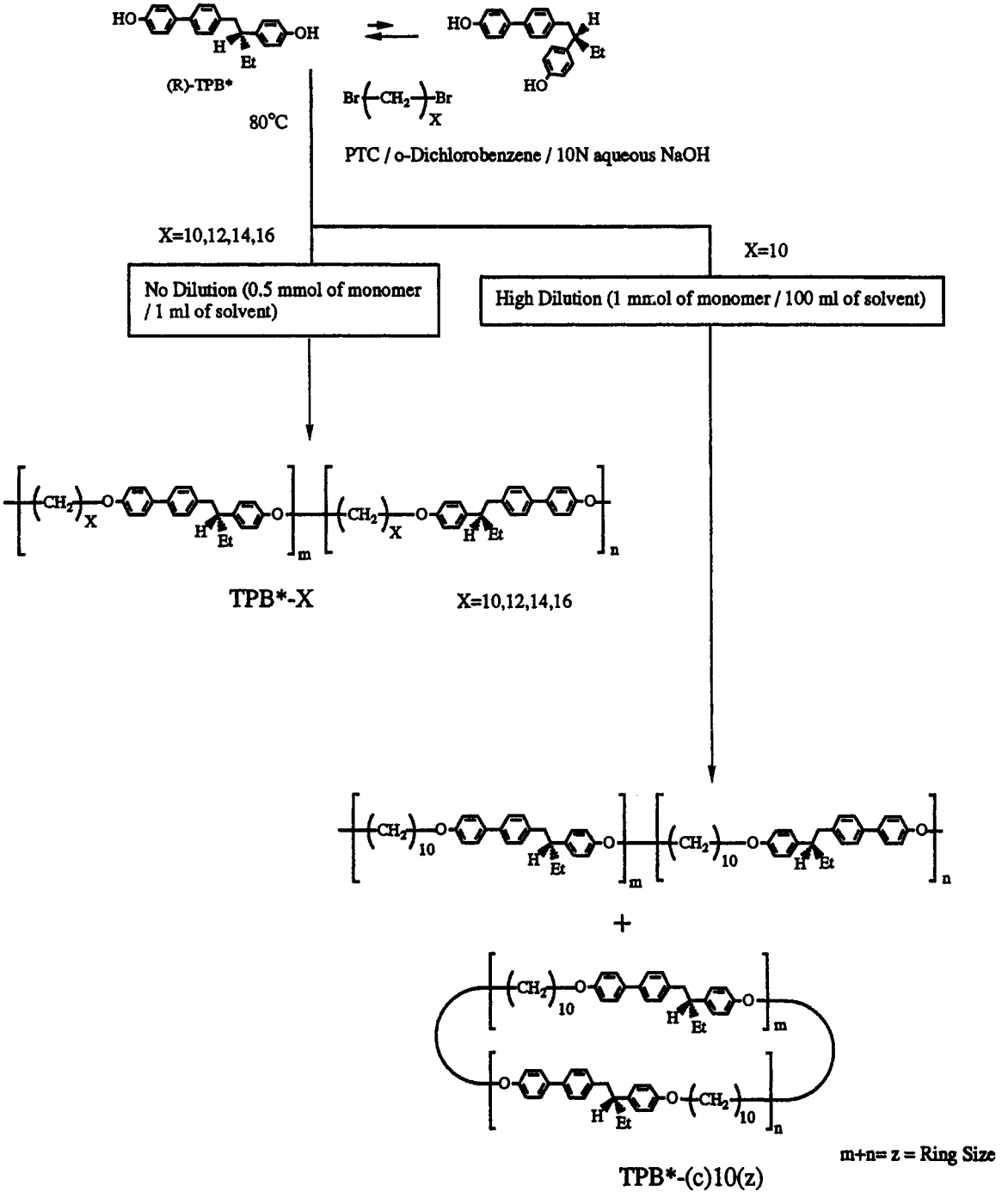

were higher than 24 000 and are comparable with the molecular weights of racemic polymers (M_n = 30 200–42 600) which were discussed in a previous paper.[9a] In addition, in this range of molecular weights the phase transition temperatures of TPB-(l)*X* are independent on the molecular weight of the polymer.[9c] Therefore, a quantitative discussion of the influence of chirality on the phase transitions of various polymers can be made. It is very important to mention at this point that, for a quantitative discussion, the linear polymers should be absolutely free of macrocyclics. This was accomplished as described in the Experimental Section, and the absence of cyclics in the linear polymer was demonstrated by GPC.

Figure 2 presents the GPC chromatograms of the reaction mixture obtained from the cyclization reaction and of the individual chiral cyclic oligomers. The purity of each cyclic oligomer is higher than 92%. The assignment of each ring size was made on the basis of the molecular weight obtained by GPC (Table II) and the linear dependence between molecular weight and elution volume. Figure 3 presents the ^{1}H-NMR spectra of the cyclic oligomers and of the high molecular weight part eluted with $CHCl_3$. No differences were observed between the spectra of the racemic cyclic oligomers and of the chiral cyclic oligomers.[9a] These spectra proved the cyclic nature of these oligomers since no terminal groups are present in these spectra, except for the case of the high molecular weight part eluted with chloroform. In addition, the chemical shifts of macrocyclics are strongly dependent on ring size. A detailed discussion on the characterization of these macrocyclics by a combination of 1D-^{1}H- and 2D-^{1}H-NMR spectroscopies and of the dependence of the chemical shift on ring size was already reported in a previous publication.[9a] The high molecular weight fraction

Table I. Characterization of Chiral Linear Polyethers Based on Chiral (*R*)-TPB and α,ω-Dibromoalkanes [(*R*)-TPB-(l)*X*] with Different Numbers of Methylene Units (*X*) and Comparison with the Corresponding Racemic Linear Polymers [TPB-(l)*X*]

polymer	yield (%)	$(M_n)_{GPC}$	$(M_w/M_n)_{GPC}$	thermal transitions (°C) and corresponding enthalpy changes (kcal/mru) in parentheses[a] heating	cooling
(*R*)-TPB(l)10	98.8	29 400	1.98	g 44 ch 56 (–0.53) ch 110 (2.58) i g 42 ch 110 (2.56) i	i 97 (2.59) ch 36 g
TPB-(l)10	99.0	37 700	2.22	g 42 k 48 n 112 (2.54) i g 43 n 112 (2.54) i	i 96 (2.61) n 35 g
(*R*)-TPB-(l)12	97.5	31 800	2.08	g 41 ch 60 (0.24) ch 102 (2.76) i g 38 ch 55 (–0.03) k 66 (0.03) ch 102 (2.64) i	i 89 (2.70) ch 31 g
TPB-(l)12	99.9	42 600	2.38	g 45 k 59 (0.39) n 65 (–0.28) n 104 (2.56) i g 39 k 69 n 104 (2.56) i	i 88 (2.69) n 31 g
(*R*)-TPB-(l)14	91.0	24 600	2.26	g 38 k 49 (0.26) 57 (–0.84) k 81 ch 95 (4.44[b]) i g 54 k 81 ch 94 (4.73[b]) i	i 83 (2.94) ch 58 (1.37) k 46 g
TPB-(l)14	92.4	30 200	2.16	38 k 58 (0.26) k 64 (–0.34) k 84 n 96 (3.97[b]) i g 49 k 85 (1.83) n 96 (2.57) i	i 83 (2.71) n 60 (1.85) k 43 g
(*R*)-TPB-(l)16	91.7	27 600	2.10	g 38 k 47 (0.22) 57 (–0.87) k 93 (5.09) i g 53 k 93 (6.24) i	i 79 ch 70 (6.36[b]) k 48 g
TPB-(l)16	93.5	33 900	2.22	g 36 k 58 k 96 (4.07[b]) i g 54 k 97 (6.50) i	i 79 (3.17) n 72 (3.13) k 41 g

[a] Data on the first line are from the first heating and cooling scans. Data on the second line are from the second heating scan. [b] Overlapped peaks.

Table II. Characterization of Chiral Cyclic (*R*)-TPB-(c)10(*z*) Oligomers (*z* Defines the Ring Size) Based on (*R*)-TPB and 1,10-Dibromodecane and Comparison with the Corresponding Racemic TPB-(c)10(*z*) Oligomers

macrocycle	yield (%)	purity by GPC (%)	MW by GPC at the peak top measd	MW by GPC at the peak top calcd	thermal transitions (°C) and corresponding enthalpy changes (kcal/mru) in parentheses[a] heating	cooling
(*R*)-TPB-(c)10(1)	6.5	98.5	566	457	g –10 i g –10 i	i –10 g
TPB-(c)10(1)	2.4	99	542	457	g –10 i g –10 i	i –10 g
(*R*)-TPB-(c)10(2)	2.5	95.9	1211	913	g 50 k 63 k 79 (–0.95[b]) k 114 (4.56) i g 24 ch 43 (0.13) i 75 (–0.36) k 110 k 125 (0.36[b]) i	i 38 (0.12) ch 19 g
TPB-(c)10(2)	3.6	92	1154	913	g 53 k 90 k 113 (5.78[b]) i g 23 n 46 (0.15) i	i 41 (0.08) n 17 g
(*R*)-TPB-(c)10(3)	1.5	94.9	1858	1370	g 37 ch 94 (0.33) i g 34 ch 94 (0.34) i	i 89 (0.37) ch 29 g
TPB-(c)10(3)	1.6	95	1845	1370	g 37 k 63 (1.19) n 95 (0.27) i g 32 n 94 (0.32) i	i 87 (0.32) n 28 g
(*R*)-TPB-(c)10(4)	0.6	92.4	2556	1827	g 37 k 64 k 83 (–2.13[b]) k 130 (3.25) i g 33 ch 128 (1.44) i	i 124 (1.29) ch 28 g
TPB-(c)10(4)	2.3	96	2343	1827	g 50 k 55 k 82 k 121 n 130 (3.13[b]) i g 29 n 127 (1.21) i	i 124 (1.18) n 25 g
(*R*)-TPB-(c)10(5)	0.7	93.4	3027	2283	g 42 ch 124 (1.28) i g 39 ch 124 (1.40) i	i 120 (1.38) ch 32 g
TPB-(c)10(5)	0.8	*d*	3100	2283	g 36 k 45 (0.09) n 127 (1.21) i g 33 n 128 (1.14) i	i 123 (1.19) n 26 g
(*R*)-TPB-(c)10(*z*) $CHCl_3$ eluted part	25.4	41[c]	$M_n = 8.81 \times 10^3$ $M_w/M_n = 1.68$		g 49 ch 54 (–0.41) ch 105 (2.48) i g 39 ch 105 (2.39) i	i 100 (2.32) ch 33 g
TPB-(c)10(*z*) $CHCl_3$ eluted part		50[c]	$M_n = 11.8 \times 10^3$ $M_w/M_n = 1.53$		g 49 k 57 k 71 n 97 (2.69[b]) i g 28 n 98 (2.31) i	i 89 (2.45) n 24 g

[a] Data on the first line are from the first heating and cooling scans. Data on the second line are from the second heating scan. [b] Overlapped peaks. [c] Mole % of cyclic polymers. [d] It contains trimer, tetramer, and higher cyclics. However, each cyclic is overlapped severely and the exact purity could not be determined.

($CHCl_3$ eluted part) obtained from the cyclization experiment exhibits a few minor peaks in the ^{1}H-NMR spectra which were attributed to terminal groups such as $-CH_2-CH=CH_2$ (resonances at 5.0 ppm for $=CH_2$) and $-CH_2-OH$ (3.6 ppm). On the basis of the integration results of these terminal groups versus the protons of the main chain groups in the NMR spectra and by using the number average molecular weight obtained by GPC, it was calculated that about 41 mol % of the high molecular weight part separated from this cyclization experiment should represent macrocyclics. This is only an estimate since the molecular weights measured by GPC are relative to polystyrene standards.

Comparison of the Phase Behavior of Racemic and Chiral Compounds. The DSC thermograms obtained from the first heating, second heating, and first cooling scans of (*R*)-TPB-(l)*X* with *X* = 10, 12, 14, and 16 are compared with those of the corresponding racemic TPB-(l)*X* polymers in Figure 4a–c. The thermal transitions and thermodynamic parameters obtained from these DSC traces are summarized in Table I. As observed from Figure 4, racemic TPB-(l)10 shows a noncrystallizable enantiotropic nematic phase which is not affected by the thermal history of the sample. The ability of TPB-(l)*X* polymers to crystallize increases with increasing spacer length, and consequently, TPB-(l)16 exhibits only a monotropic

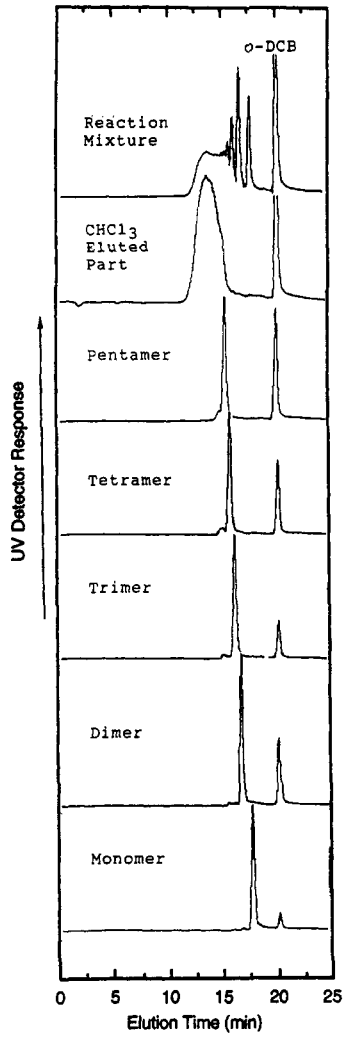

Figure 2. GPC chromatograms of the reaction mixture, of the high molecular weight part eluted with $CHCl_3$ and of the separated chiral cyclic oligomers [(*R*)-TPB-(c)10(*z*)].

nematic phase. Therefore, the effect of chirality of the mesogenic unit can be investigated with respect to both the nematic and the crystalline phases of the resulting polymers. As clearly seen from the DSC thermograms of Figure 1 and from their thermal transitions in Table I, there are no differences between the phase behavior of chiral and racemic TPB-(l)*X* polymers except that the chiral polymers become cholesteric.

The DSC thermograms obtained from the first and second heating and from the cooling scans of (*R*)-TPB-(c)10(*z*) oligomers are compared with those of the corresponding racemic TPB-(c)10(*z*) oligomers in Figure 5. Also, the data obtained from these DSC traces are summaried together with the other analytical data in Table II. Again, there are only very slight differences between the phase behavior of chiral and racemic TPB-(c)10(*z*) oligomers. The differences are as follows. First, the melting temperature (130 °C) of the chiral tetramer is higher than that of the racemic tetramer (120 °C) while their isotropization temperatures (128 °C) are identical. Consequently, the mesophase of the tetramer is transformed from enantiotropic for the case of the racemic TPB-(c)10(4) tetramer into a monotropic mesophase for the case of chiral (*R*)-TPB-(c)10(4). Second, the enthalpy changes associated with the isotropization of the chiral tetramers and pentamers seem to be slightly higher than those of the corresponding racemic macrocyclics. During the second heating scan the chiral dimer exhibits a crystallization exotherm above the isotropization transition while the racemic dimer does not display this crystallization process. This slightly enhanced ability to crystallize in the case of the racemic macrocyclics may be attributed to a decreased entropy of the cyclic racemic compound.

Although the DSC thermograms of the chiral and racemic macrocyclics are not very different, the textures of their mesophases and their spectroscopic properties are quite different. The thin film obtained from the chiral trimer is transparent and displays a strong reflection of the purple color in the range of temperatures in which it is in the cholesteric phase. Its color changes slightly as a function of temperature. Near the isotropization temperature, it is purple and it becomes blue on cooling. This color can be retained even after cooling to room temperature. No color change was observed during 4 months at room temperature. Also, the chiral dimer reflects the blue color when its thin film was prepared by quenching from its isotropic melt. This reflection of color is due to its cholesteric structure. Therefore, the helical pitch of the cholesteric phase is close to the wavelength of visible light. The chiral tetramer and pentamer did not show such a strong color change in their cholesteric phases.

Figure 6 compares the textures exhibited by the mesophases of the chiral cyclic tetramer and racemic tetramer. The chiral tetramer displays a simple focal conic texture, while the racemic tetramer exhibits a schlieren texture. The simple focal conic texture indicates that the phase of the chiral tetramer is either cholesteric or smectic A.[13] However, the transition temperature and the enthalpy change of the chiral tetramer were similar to those of the racemic tetramer whose mesophase is nematic. Therefore, this focal conic texture is most probably attributed to a cholesteric structure since a smectic–isotropic phase transition would be accompanied by an enthalpy change much higher than that of the nematic–isotropic phase transition. The focal conic texture of the cholesteric phase is generally obtained when the cholesteric phase is strongly twisted (i.e., when the helical pitch of the cholesteric phase is very short).[13] This is consistent with the fact that the chiral tetramer does not reflect color. The chiral pentamer exhibits the focal conic texture shown in Figure 7. This cholesteric mesophase should also display a strong twist. On the other hand, as observed from Figure 8 the chiral cyclic dimer and trimer do not exhibit such a texture. It is obvious from these data that the helical pitch of the chiral cyclic oligomers is highly dependent on ring size. The linear (*R*)-TPB-(l)10 polymer exhibits only a schlieren texture which is quite similar to that of the racemic TPB-(l)10 polymer. The film of (*R*)-TPB-(l)10 polymer reflects the light blue color only when it is prepared by quenching from the isotropic melt.

Figure 9 presents the UV and CD spectra of the (*R*)-TPB, (*R*)-TPB-(c)10(*z*), macrocyclics, and (*R*)-TPB-(l)10 polymers obtained from dioxane solutions. The UV spectra of all compounds are characterized by the presence of strong absorption bands at 213–219 nm (A1) and 265–268 nm (A2). The A1 band is attributed to the π–π^* electronic transition of the phenylene ring of the mesogen, while the A2 peak is due to the π–π^* electronic transition of the biphenyl ring. All, the chiral (*R*)-TPB monomer, cyclic oligomers, and linear polymers, show negative CD signals around 260 nm. This signal is close to the UV absorption maximum corresponding to the A2 peaks (Figure 9). Also, there is a small shoulder besides the main peak. The presence of these CD signals clearly indicates that the aromatic groups in the mesogenic TPB are located in a chirally perturbed environment. However, the CD spectra do not change much with changing the

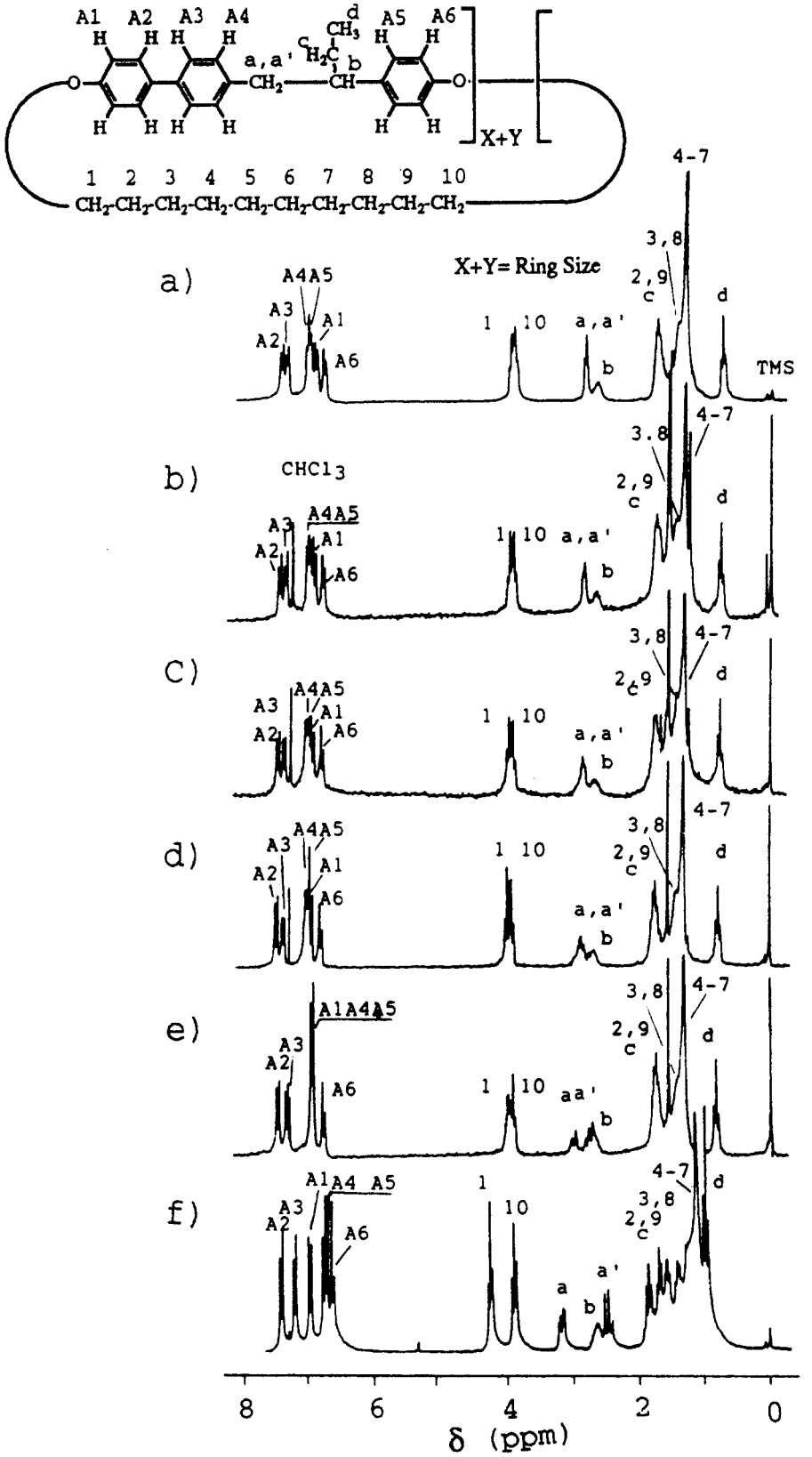

Figure 3. 200-MHz ^{1}H-NMR spectra of a chiral cyclic (*R*)-TPB-(c)10(*z*) series: (a) $CHCl_3$ eluted part; (b) cyclic pentamer; (c) cyclic tetramer; (d) cyclic trimer; (e) cyclic dimer; (f) cyclic monomer ($CDCl_3$, TMS).

ring size or architecture, except for the case of the cyclic monomer which does not present the little shoulder but only the main peak.

Figure 10 shows the CD spectra of the films of chiral (*R*)-TPB-(c)10(*z*) oligomers and chiral linear (*R*)-TPB-(l)10 polymers. The cover glass on which these films were prepared absorbs in UV below 315 nm. Therefore, these results are reliable only above 315 nm. These samples were prepared by quenching the film from the cholesteric state without shearing. All films were rotated around the axis parallel to the incident light, and no change in their spectra was observed. The cyclic dimer and trimer exhibit a very strong and broad CD signal with a peak maximum at about 330–340 nm. These peaks were not observed in the CD spectra of their corresponding solutions. Therefore, these new peaks are due to the induced chirality in

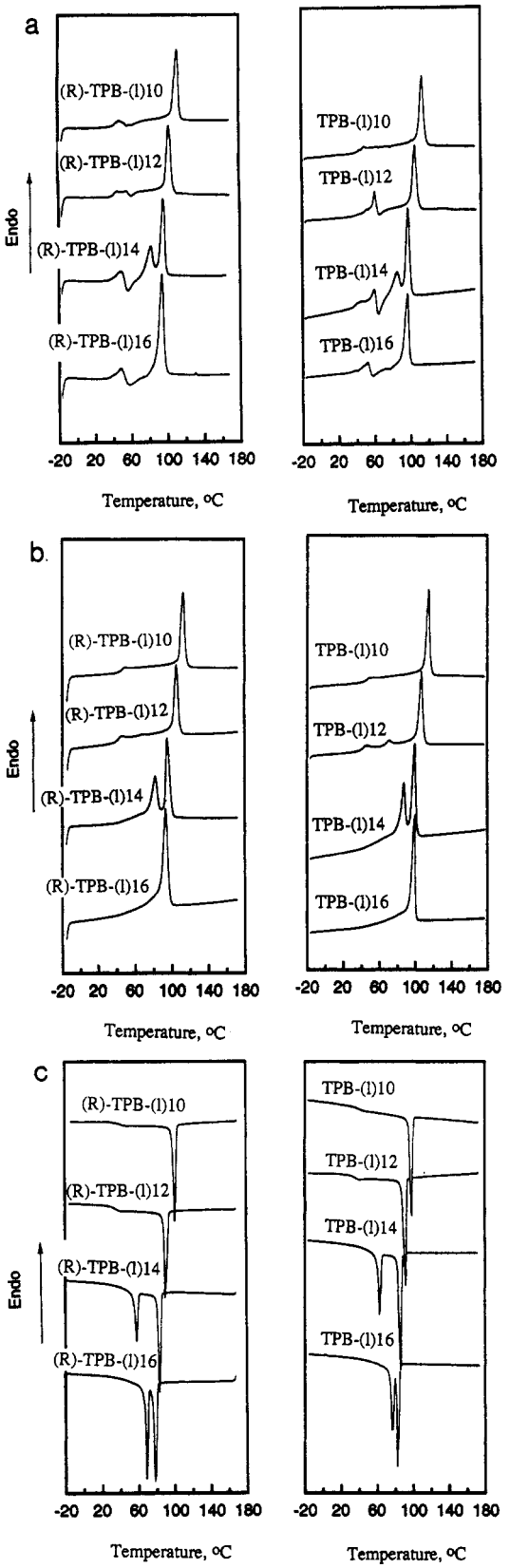

Figure 4. DSC thermograms of the chiral linear (*R*)-TPB-(l)*X* polymers and of the racemic TPB-(l)*X* polymers obtained from (a) the first heating, (b) the second heating, and (c) the first cooling scans.

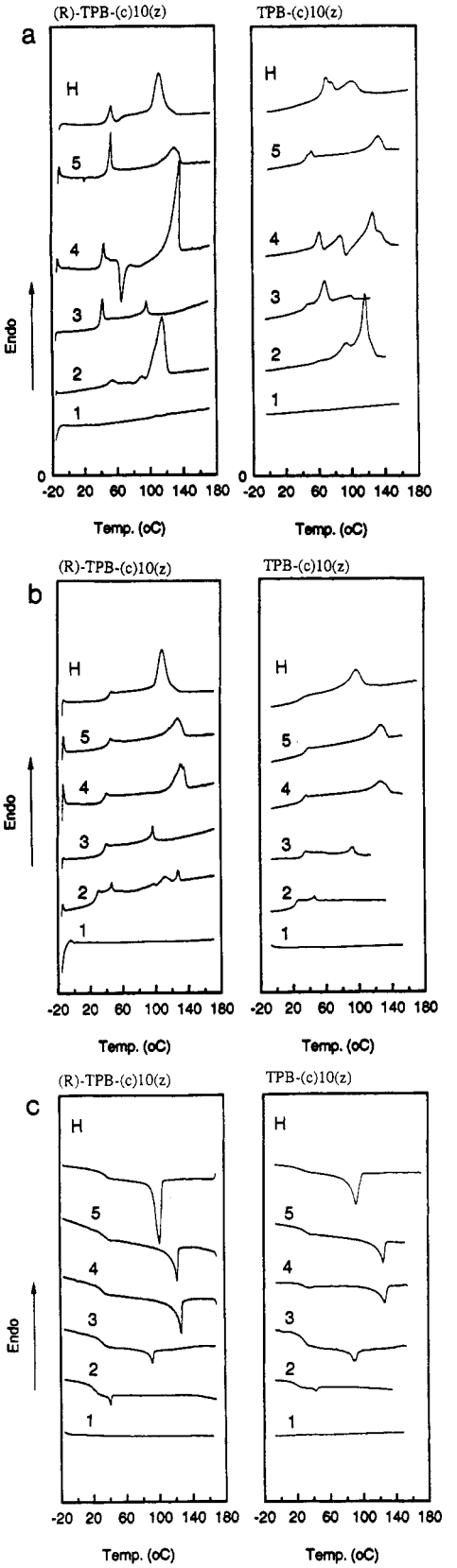

Figure 5. DSC thermograms of the chiral cyclic (*R*)-TPB-(c)10(*z*) oligomers and of the racemic cyclic TPB-(c)10(*z*) oligomers obtained from (a) the first heating (numbers on the figure indicate the ring size. H indicates the part eluted with $CHCl_3$), (b) the second heating, and (c) the cooling scans.

the supramolecular structure of the cholesteric phase. On the other hand, the cyclic tetramer and pentamer exhibit a very weak CD signal above 315 nm. The CD spectra of the tetramer and pentamer were obtained with films much thicker than those of the cyclic dimer and trimer. Also, the spectra of the tetramer and pentamer are more expanded. Therefore, the peaks of the tetramer and pentamer in Figure 10 are highly amplified. As discussed above, the tetramer and pentamer exhibit a very high twist in their cholesteric structure. This result is quite reasonable since the main CD signals should exist far below

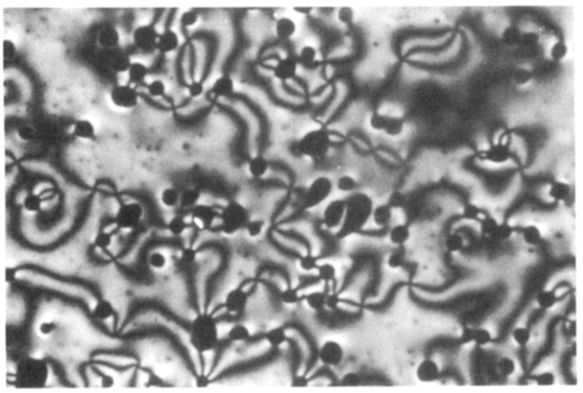

a)

b)

Figure 6. Textures of the chiral cyclic (*R*)-TPB-(c)10(*z*) tetramer and of the racemic cyclic TPB-(c)10(*z*) tetramer observed under an optical polarized microscope (×50): (a) schlieren nematic texture of a racemic tetramer at 114.3 °C on heating; (b) focal conic cholesteric texture of a chiral tetramer after annealing at 115.9 °C for 3 min.

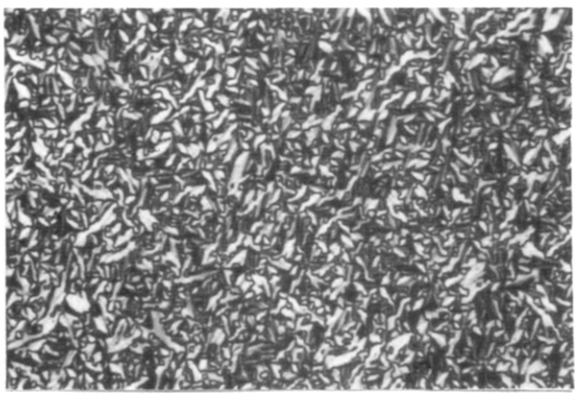

Figure 7. Texture of a chiral cyclic (*R*)-TPB-(c)10(*z*) pentamer observed under an optical polarized microscope (×50) (annealing at 111.4 °C for 2 min).

the region where the spectrum was measured. On the other hand, the linear polymer exhibits only a very broad negative CD signal with a peak maximum at 430 nm.

Although according to these CD experiments the chirality of the cyclic oligomers and linear polymers is quite similar in solution, in the solid state, there is a drastic change in the helical pitch. These observations strongly suggest that the cyclic tetramer and pentamer have an enhanced chirality of their suprastructure in the mesomorphic state compared to that of the dimer, trimer, and linear polymer. One possible suprastructure of the tetramer and pentamer is a supercoiled one (Chart I) similar to that of cyclic DNA.[14] The supercoiled structure itself

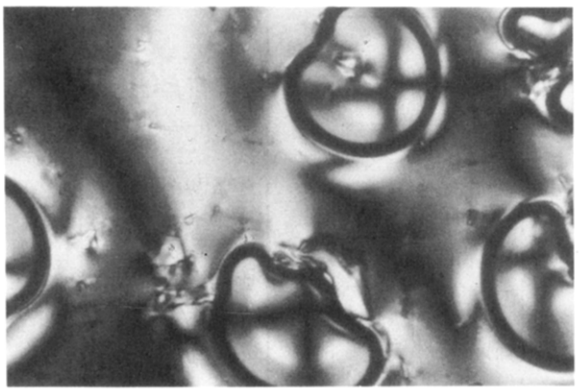

a)

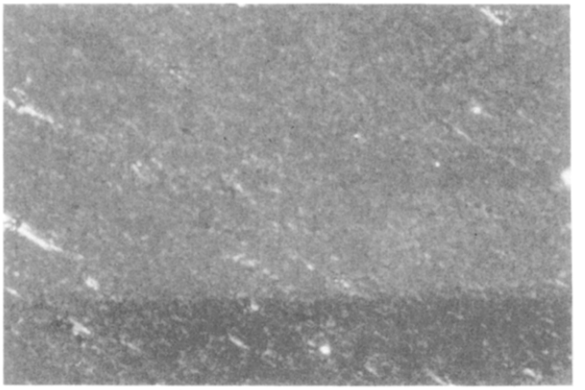

b)

Figure 8. Textures of a chiral cyclic (*R*)-TPB-(c)10(*z*) dimer and trimer observed under an optical polarized microscope (×50): (a) the cyclic dimer quenched from isotopic melt; (b) the cyclic trimer after annealing at 86 °C for 2 min.

has a higher chirality due to its secondary coiled structure and may cause a stronger twist of the mesophase. Elucidation of the suprastructure of these cyclic oligomers is required in order to confirm this speculative explanation.

Interpretation of the Phase Behavior of Irregular Linear and Macrocyclic Compounds Based on the Absence of Chiral Molecular Recognition. Stereochemistry is the most sensitive tool for probing the structural details or how molecules "see" each other as they come together to form complexes and transition states and, therefore, represents the most powerful tool available in chemistry for the study and manipulation of molecular shapes and symmetry properties.[15]

The most notable series of investigations in this field refers to the study of chiral molecular recognition in monolayers of pure enantiomers and their pairs as well as in monolayers of pure diastereomers and their mixtures.[15a,16] Enantiomers are considered to be perfect physical and chemical models for each other since their properties are identical, except those that involve their interactions with other chiral systems. Chiral discrimination between the properties of monolayers formed by pure enantiomers and their mixtures (i.e., enantiomeric interaction) was always observed, with the notable exception of phosphatidylcholine.[17] In the field of molecular thermotropic liquid crystals there are only few examples in which the phase diagrams of binary mixtures of enantiomeric compounds were investigated.[15c,18] In two of these cases,[18a,e] it has been observed that enantiomeric recognition occurs and it increases the mesomorphic transition temperature of the racemic mixture by comparison with those of the pure enantiomers.

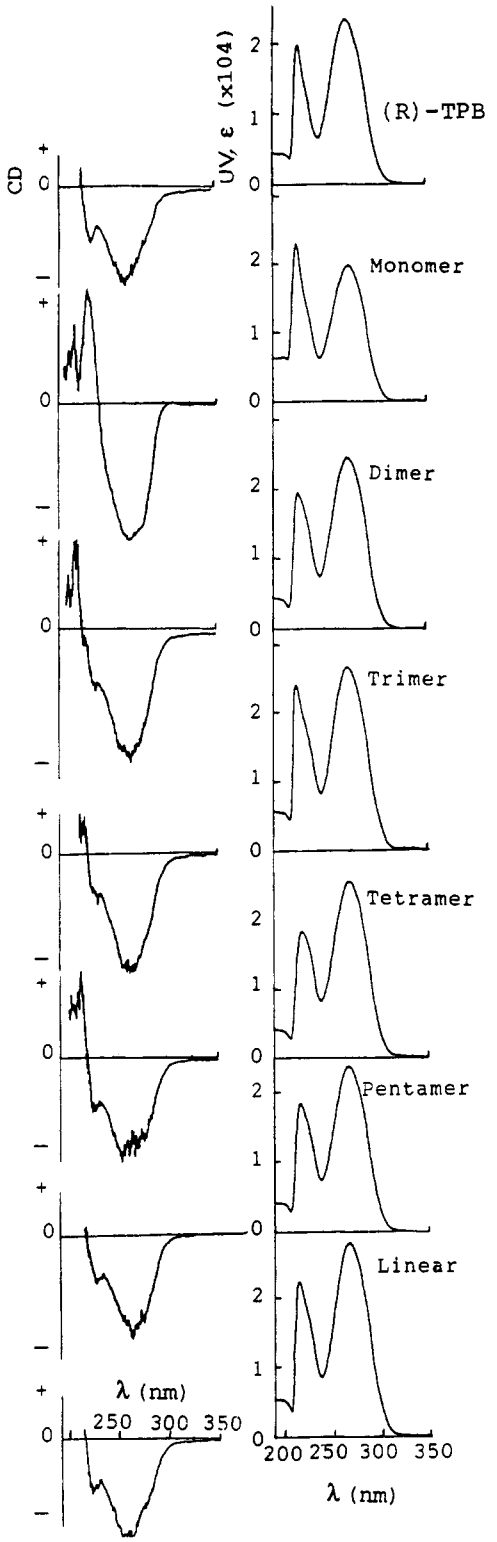

Figure 9. UV and CD spectra of the dioxane solutions of (*R*)-TPB, the chiral (*R*)-TPB-(c)10(*z*) oligomers, and the chiral linear (*R*)-TPB-(l)10 polymers.

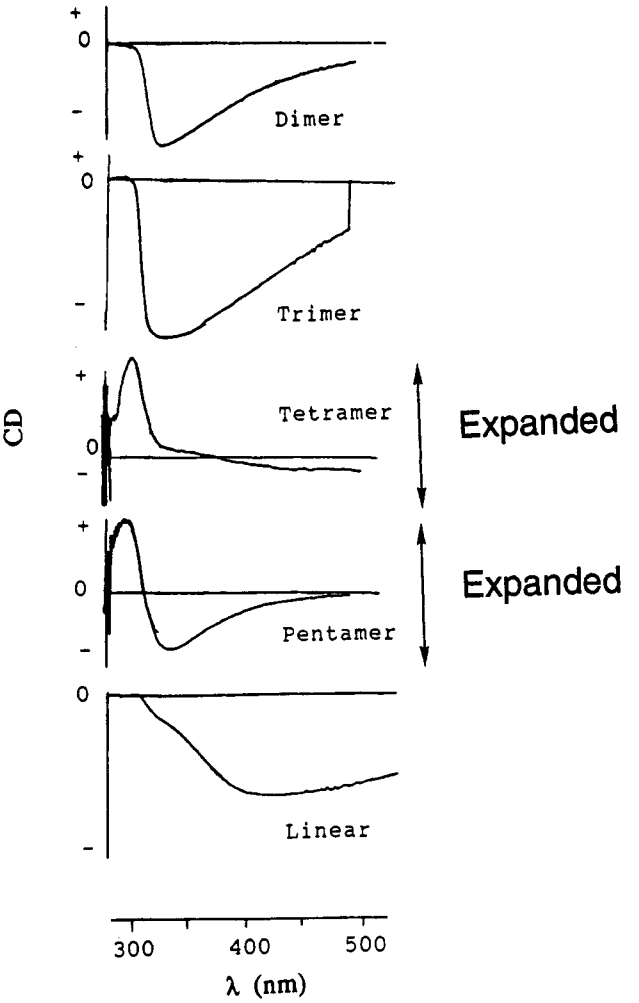

Figure 10. CD spectra of the films of chiral (*R*)-TPB-(c)10(*z*) oligomers and of the chiral linear (*R*)-TPB-(l)10 polymers. (The films of the tetramer and pentamer are much thicker than those of the dimer, trimer, and linear polymer. Also the *y*-axes of the tetramer and pentamer spectra are more expanded.)

Chart I. Supercoiled Structure Suggested for the Chiral (*R*)-TPB-(c)10(*z*) Tetramer and Pentamer

In summary, chiral molecular recognition in mixtures and in copolymers of enantiomers takes place only when the two enantiomers are isomorphic, or in other words, when they behave as an ideal solution, and should be judged independently for each phase in part.[19] Isomorphism is quite often encountered in a common mesophase of liquid crystalline compounds. However, this is not the case for their crystalline phases.[19] Therefore, the most common case of chiral molecular recognition between two enantiomers is expected to exhibit a positive deviation of the dependence of temperature transitions of the various mesophases as a function of enantiomeric composition with a maximum for the racemic mixture.[15c,18e] This behavior corresponds to a positive deviation of the phase transition temperatures from the Schroeder–van Laar equation. Nevertheless, the melting temperatures of these mixtures and copolymers are expected to be suppressed and exhibit a eutectic composition.[19,20]

The phase behavior of chiral and racemic irregular polyethers described in this paper is, within experimental error, identical (Table I). This demonstrates that the enantiomeric structural units of the linear polymers are isomorphic both in their liquid crystalline and in their crystalline phases. However, since the transition temperatures associated with the liquid crystalline and crystalline phases of the racemic polyethers are identical with those of the chiral polyethers it means that there is no chiral molecular recognition in any of these two phases.

In the case of macrocyclics, we can consider that within the accuracy of our experiments, the isotropization temperatures of chiral compounds are identical to those of the racemic compounds. However, chiral macrocyclics do display a higher ability to crystallize than the racemic compounds (Table II). These data can be interpreted in the following way. The enantiomeric structural units of all macrocyclics are isomorphic within their liquid crystalline phase but not in their crystalline phases. Therefore, while isotropization temperatures of the chiral compounds are identical with those of the racemic compounds, the melting temperatures of the chiral compounds are higher than those of the racemic compounds. As a consequence, the chiral tetramer is monotropic while the racemic tetramer is enantiotropic. Again, absence of chiral recognition in both phases is responsible for the phase behavior of chiral and racemic macrocyclics.

Most probably, the absence of chiral recognition in the linear and racemic compounds reported in this paper is due to their irregular microstructure. In the absence of chiral molecular recognition, the dependence of the CD spectrum in the mesomorphic phase of macrocyclics on ring size is even more rewarding.

Conclusions

Chiral linear (*R*)-TPB-(l)*X* polymers and cyclic (*R*)-TPB-(c)10(*z*) oligomers were synthesized and characterized. The chiral polymers and oligomers exhibit a phase behavior almost similar to that of the racemic polymers and oligomers. A detailed comparison of these data demonstrated the absence of chiral molecular recognition within both the liquid crystalline and crystalline phases of both linear and macrocyclic compounds. From the investigation of the textures and the results of solid state CD experiments, it was suggested that the chirality of the mesophase displayed by macrocyclics is highly dependent on the ring size and the suprastructure of the molecule. On the basis of these results a supercoiled suprastructure was suggested for the macrocyclic tetramer and pentamer.

Acknowledgment. Financial support by the National Science Foundation, Polymers Program (DMR-92-06781), and Toyota Central R & D Laboratories, Japan, is gratefully acknowledged.

References and Notes

(1) (a) This is Part 31 in the series "Liquid Crystalline Polyethers Based on Conformational Isomersm"; for Part 30 in this series see ref 10g. (b) Soladie, G.; Gottarelli, G. *Tetrahedron* **1987**, *43*, 1425.

(2) Percec, V.; Jonsson, H.; Tomazos, D. In *Polymerization in Organized Media*; Paleos, C. M., Ed.; Gordon and Breach Science Publishers: Philadelphia, 1992; p 1.

(3) (a) Saeva, F. D., Ed. *Liquid Crystals. The Fourth State of Matter*; Marcel Dekker: New York, 1979. (b) Chiellini, E.; Galli, G. In *Recent Advances in Liquid Crystalline Polymers*; Chapoy, L. L., Ed.; Elsevier Science Publishing: New York, 1985; p 15. (c) Shibaev, V. P.; Freidzon, Ya. S. In *Side Chain Liquid Crystal Polymers*; McArdle, C. B., Ed.; Chapman and Hall: New York, 1989; p 130.

(4) (a) Goodby, J. W. *Science* **1986**, *231*, 350. (b) Goodby, J. W. *J. Mater. Chem.* **1991**, *1*, 307. (c) Goodby, J. W., Ed. *Ferroelectric Liquid Crystals. Principles, Properties and Applications*; Gordon and Breach Science Publishers: Philadelphia, 1991. (d) LeBarny, P.; Dubois, J. C. In *Side Chain Liquid Crystal Polymers*; McArdle, C. B., Ed.; Chapman and Hall: New York, 1989; p 130. (e) Escher, C.; Wingen, R. *Adv. Mater.* **1992**, *4*, 189.

(5) (a) Wendorff, J. H. *Angew. Chem., Int. Ed. Engl.* **1991**, *30*, 405. (b) Meier, W.; Finkelmann, H. *Makromol. Chem. Rapid Commun.* **1990**, *11*, 599. (c) Vallerien, S.; Kremer, F.; Fisher, E. W.; Kapitza, H.; Zentel, R.; Poths, H. *Makromol. Chem. Rapid. Commun.* **1990**, *11*, 593.

(6) (a) Naikwadi, K. P.; McGovern, A. M.; Karasek, F. W. *Can. J. Chem.* **1987**, *65*, 970. (b) Aggarwal, S. K.; Bradshaw, J. S.; Eguchi, M.; Parry, S.; Rossiter, B. E.; Markides, K. E.; Lee, M. L. *Tetrahedron* **1987**, *43*, 451.

(7) (a) Ciardelli, F.; Salvadori, P. *Pure Appl. Chem.* **1985**, *57*, 931. (b) Selegny, E., Ed. *Optically Active Polymers*; D. Reidel Publishing Co.: Dordrecht, The Netherlands, 1979. (c) Matsuzaki, K.; Watanabe, T. *Makromol. Chem.* **1971**, *146*, 109.

(8) (a) van Luyen, D.; Liebert, L.; Strzelecki, L. *Eur. Polym. J.* **1980**, *16*, 307. (b) Vilasagar, S.; Blumstein, A. *Mol. Cryst. Liq. Cryst., Lett. Sect.* **1980**, *56*, 203. (c) Krigbaum, W. R.; Ciferri, A.; Asrar, J.; Toriumi, H.; Preston, J. *Mol. Cryst. Liq. Cryst.* **1981**, *76*, 79. (d) Park, H. J.; Jin, J. Il.; Lenz, R. W. *Polymer* **1985**, *26*, 1301. (e) Watanabe, J.; Krigbaum, W. R. *J. Polym. Sci., Polym. Phys. Ed.* **1985**, *23*, 565. (f) Moore, J. S.; Stupp, S. I. *J. Am. Chem. Soc.* **1992**, *114*, 3429. (g) Fujishiro, K.; Lenz, R. W. *Macromolecules* **1992**, *25*, 81 and 85.

(9) (a) Percec, V.; Kawasumi, M. *Macromolecules* **1991**, *24*, 6318. (b) Schneider, A.; Blackwell, J.; Chvalun, S.; Hofman, D.; Ungar, G.; Kawasumi, M.; Percec, V. Manuscript in preparation. (c) Percec, V.; Kawasumi, M. *Macromolecules*, in press. (d) Gu, D.; Jamieson, A. M.; Kawasumi, M.; Lee, M.; Percec, V. *Macromolecules* **1992**, *25*, 2151. (e) Gu, D.; Jamieson, A. M.; Lee, M.; Kawasumi, M.; Percec, V. *Liq. Cryst.* **1992**, *12*, 961.

(10) (a) Percec, V.; Kawasumi, M.; Rinaldi, P. L.; Litman, V. E. *Macromolecules* **1992**, *25*, 3851. (b) Percec, V.; Kawasumi, M. *Adv. Mater.* **1992**, *4*, 572. (c) Percec, V.; Kawasumi, M. *Liq. Cryst.* **1993**, *13*, 83. (d) Percec, V.; Kawasumi, M. *Mol. Cryst. Liq. Cryst.*, in press. (e) Percec, V.; Kawasumi, M. *Chem. Mater.*, in press. (f) Percec, V.; Kawasumi, M. *J. Mater. Chem.*, in press. (g) Percec, V.; Kawasumi, M. *J. Chem. Soc., Perkin Trans 1*, in press.

(11) Percec, V.; Tsuda, Y. *Macromolecules* **1990**, *23*, 3509.

(12) Aaron, C.; Dull, D.; Schmiege, J. L.; Jaeger, D.; Ohashi, Y.; Mosher, H. S. *J. Org. Chem.* **1967**, *32*, 2797.

(13) Demus, D.; Richter, L. *Textures of Liquid Crystals*; Verlag Chemie: Weinheim, 1978.

(14) Scovell, W. M. *J. Chem. Educ.* **1986**, *63*, 562.

(15) (a) Arnett, E. M.; Harvey, N. G.; Rose, P. L. *Acc. Chem. Res.* **1989**, *22*, 131. (b) Pirkle, W. H.; Pochapsky, T. P. *Chem. Rev.* **1989**, *89*, 347. (c) Jacques, J.; Collet, A.; Wilen, S. H. *Enantiomers, Racemates and Resolutions*; Krieger Publishing Co.: Malabar, FL, 1991.

(16) (a) Arnett, E. M.; Thompson, O. *J. Am. Chem. Soc.* **1981**, *103*, 968. (b) Harvey, N. G.; Rose, P. L.; Mirajovsky, D.; Arnett, E. M. *J. Am. Chem. Soc.* **1990**, *112*, 3547.

(17) Arnett, E. M.; Gold, J. M. *J. Am. Chem. Soc.* **1982**, *104*, 636.

(18) (a) Leclercq, M.; Billard, J.; Jacques, J. *Mol. Cryst. Liq. Cryst.* **1969**, *8*, 367. (b) Yamada, Y.; Mori, K.; Yamamoto, N.; Hayashi, H.; Nakamura, K.; Yamawaki, M.; Orihara, H.; Ishibashi, Y. *Jpn. J. Appl. Phys.* **1989**, *28*, L 1606. (c) Takezoe, H.; Fukuda, A.; Ikeda, A.; Takanishi, Y.; Umemoto, T.; Watanabe, J.; Iwane, H.; Hara, M.; Itoh, K. *Ferroelectrics* **1991**, *122*, 167. (d) Takezoe, H.; Lee, J. I.; Chandani, A. D. L.; Gorecka, E.; Ouchi, Y.; Fukuda, A.; Terashima, K.; Furukawa, K. *Ferroelectrics* **1991**, *114*, 187. (e) Slaney, A. J.; Goodby, J. W. *Liq. Cryst.* **1991**, *9*, 849.

(19) For a general discussion on isomorphism in molecular and macromolecular liquid crystals see: Percec, V.; Tsuda, Y. *Polymer* **1991**, *32*, 661.

(20) For general discussions on the application of the Schroeder–van Laar equation to molecular and macromolecular liquid crystals see: (a) Percec, V.; Tomazos, D. In *Comprehensive Polymer Science*; Allen, Sir G., Ed.; Pergamon Press: Oxford, U.K., 1992; First Suppl., pp 300–383. (b) Percec, V.; Tomazos, D. *Adv. Mater.* **1992**, *4*, 548. (c) Van Hecke, G. R. *J. Phys. Chem.* **1979**, *83*, 2344. (d) Achard, M. F.; Mauzac, M.; Richard, M.; Sigaud, M.; Hardouin, F. *Eur. Polym. J.* **1989**, *25*, 593.